

Dynamic Power Allocation For NOMA-Based Transmission in 6G Optical Wireless Networks

Ahmad Adnan Qidan, Taisir El-Gorashi, Majid Safari, Senior Member, IEEE, Harald Haas, Fellow, IEEE, Richard V. Penty, Fellow, IEEE, Ian H. White, Fellow, IEEE, and Jaafar M. H. Elmirghani, Fellow, IEEE

Abstract—Optical wireless communication (OWC) has been considered as a key enabling technology to unlock unprecedented speeds of communication, supporting high demands of data traffic. In this paper, infrared lasers are used as optical transmitters operating in an indoor environment under eye safety regulations due to their high modulation speed. To provide efficient multiple access service, non-orthogonal multiple access (NOMA)-based transmission is implemented to multiplex messages intended to multiple users in the power domain and maximize the spectral efficiency of our laser-based OWC network. In particular, a blind interference alignment (BIA) outer precoder is designed to coordinate the transmission among multiple optical access points (APs) and determine the precoding matrices for groups of users potential formed according to NOMA principles. For effective use of NOMA, an optimization problem is formulated to maximize the sum rate of the network through forming optimum groups under certain joint conditions, efficient power allocation, high quality of service for each weak and strong users, and high overall system performance. Such optimization problems are defined as max-min fractional programs difficult to solve in practice. Therefore, a dynamic application for NOMA is introduced using two algorithms. First, a Radio frequency (RF)-aided dynamic algorithm is designed to form multiple groups, where users exchange binary variables among them through an RF system to establish distance-based weight edges, which are used as a metric for the grouping process. Second, a dynamic power allocation is proposed to determine the optimum power allocated to each group, while the users belonging to a certain group receive their traffic demands regardless of their classification as weak or strong. The results show the convergence of the proposed dynamic application to the optimum solution, and its high performance in terms of sum rate, fairness, and energy efficiency compared to counterpart schemes.

Index Terms—Optical wireless communications, NOMA, laser-based transmission, interference management, power allocation, dynamic optimization

I. INTRODUCTION

Ahmad Adnan Qidan, Taisir E. H. El-Gorashi and Jaafar M. H. Elmirghani are with Department of Engineering, Faculty of Natural, Mathematical and Engineering Sciences, King's College London, London, United Kingdom (UK). (e-mails: ahmad.qidan@kcl.ac.uk; taisir.elgorashi@kcl.ac.uk; jaafar.elmirghani@kcl.ac.uk)

Majid Safari is with the School of Engineering, Institute for Digital Communications, The University of Edinburgh, Edinburgh, UK. (e-mail: majid.safari@ed.ac.uk).

Harald Haas is with the LiFi Research and Development Centre (LRDC), Electrical Engineering Division, Department of Engineering, University of Cambridge, Cambridge, UK. (e-mail: huh21@cam.ac.uk).

Richard V. Penty is with the Centre for Photonic Systems, Electrical Engineering Division, Department of Engineering, University of Cambridge, Cambridge, UK. (e-mail: rvp11@cam.ac.uk).

Ian H. White is with the University of Bath, Bath, UK. (e-mail: i.h.white@bath.ac.uk).

Optical wireless communication (OWC) is a well-known technology that have been investigated to support various next-generation (6G and beyond) applications operating at high data rates in a range of gigabit per second (Gbps). In [1], light-emitting diodes (LEDs) were used in indoor environments to provide illumination and communication at high speeds. Interestingly, OWC systems have several advantages including the provision of high spectral and energy efficiency, low cost-infrastructure and low power consumption compared to Radio frequency (RF) networks. However, LED-based OWC systems have limited modulation speeds, and sending information at high communication speeds might affect the illumination function of the LED. Given that, infrared lasers, such as vertical-cavity surface-emitting(VCSEL) lasers, have received enormous interest as a strong candidate in the next generation of OWC due to their small size, long life time and high modulation speed. An IR laser provides usually uniform illumination within a small and confined coverage area in a range of a few square centimeters. However, an array of IR lasers can be designed to expand the coverage area to a few square meters. In an indoor environment, multiple IR laser arrays operating under eye safety regulations are needed to ensure uniform coverage and seamless transition for multiple users on the floor [2], [3], [4].

In OWC, multi-user interference management is a crucial issue that plays a major role in determining the spectral efficiency of the network. Recently, non-orthogonal multiple access (NOMA) has been considered as a promising approach to serve a high number of users simultaneously over the same resources, i.e., frequency or time slots, compared to orthogonal schemes [5], [6], [7], [8]. Basically, the implementation of NOMA in wireless networks requires user-classification algorithms that form groups of strong and weak users to exploit the power domain by assigning a different power level to each user based on their channel gains. In [9], NOMA was applied in an OWC network considering realistic indoor optical channel conditions. In [10], the performance of NOMA was evaluated in OWC networks under the guarantee of high quality of service (QoS). Furthermore, the evaluation of bit-error-rate (BER) in NOMA-based OWC systems was addressed in [11], deriving a closed-form expression taking into account interference cancellation errors. In [12], the performance of NOMA was investigated in multiple-input multiple-output (MIMO) OWC systems, serving multiple users at high sum rates. It was shown that NOMA achieves higher data rates dictated by power allocation and the difference in channel gain between weak and strong users.

A. Related Works

The application of NOMA to manage multi-user interference in wireless networks is subject to two main challenges. First, inter-group interference, which means that after dividing the users into several groups, each user suffers interference received due to transmission to the adjacent groups, resulting in significant degradation in the signal to interference and noise ratio (SINR). For instance, in [13], NOMA was applied in MIMO RF networks considering the case of multiple group generating interference among them. To eliminate this interference, it is proposed that the users of each group are served using a unique transmit beamforming vector, which involves high cost in terms of complexity. In [14], a robust beamforming was also designed for NOMA to serve multiple clusters of users in a multiple-input-single-output (MISO) RF setup under errors in channel estimation. OWC networks differ than RF networks in terms of density and the characteristics of the transmitted signal. Therefore, the implementation of such beamforming techniques in OWC might lead to complex optimization problems, hence, orthogonal transmission between clusters of users was considered in [15] and the majority of the NOMA-related work in OWC, compromising on overall system performance. Second issue in the application of NOMA especially in OWC networks is that each optical AP illuminates a small area referred to as attocell, and each group of users might experience low SNR due to inter-cell interference. In [16], NOMA was used to serve users in a multi-cell OWC network, where a user-grouping algorithm is designed to determine user combinations taking into account their locations, while frequency reuse (FR) was applied among the cells to avoid inter-cell interference. However, an indoor environment usually contains a high number of optical APs, and therefore, managing each optical AP independently causes severe inter-cell interference. Moreover, using a frequency reuse technique in such high density scenarios is insufficient, and users might be subject to handover every few centimeters in dynamic OWC networks [17].

At this point, a transmission scheme referred to as blind interference alignment (BIA) was proposed in [18] to coordinate the transmission among RF transmitters and manage multi-user interference. Basically, the transmission block of BIA allocates alignment blocks from the transmitters to each user following a certain methodology. In this case, each user must have the ability to switch its reception modes over its allocated alignment blocks following a predefined pattern. It was shown that a unique antenna, namely reconfigurable antenna, is needed for providing a set of radiation patterns from the transmitters and enabling the application of BIA in RF networks. It is worth mentioning that the size of transmission block of BIA increases with the number of transmitters and users, and therefore, the channel coherence time must be large enough to guarantee the delivery of such transmission blocks with minimum errors. In [19], the methodology of BIA was adopted to manage inter-group interference rather than multi-user interference in RF networks, while each group contains a pair of users served using NOMA. In [20], [21], a reconfigurable optical receiver was proposed to enable

the application of BIA-based transmission in OWC, where this receiver allows the user to switch its reception modes over time, providing linearly independent channel responses from a set of optical transmitters. In [22], [23], [24], new BIA schemes were proposed with the aim of enhancing its performance in OWC networks of high density. It is worth pointing out that the application of BIA in OWC is superior compared to orthogonal or transmit precoding schemes. It is because of BIA naturally coordinates the transmission among the transmitters, while each user can measure and cancel multi-user interference. Given the features and limitations of BIA, this work adopts its application in NOMA-based OWC to overcome the limitations of NOMA in terms of inter-group interference and inter-cell interference, while exploiting the NOMA ability in providing multiple access service within a certain group.

In NOMA transmission, transmitters send information using the power domain, giving users the opportunity to exploit all the available resources. Therefore, suitable power allocation schemes are essential in NOMA. This issue has been investigated extensively in the literature in the context of RF and OWC systems. In [25], a novel gain ratio power allocation (GRPA) approach was proposed to allocate the power among the users considering their channel conditions. It was shown that the GRPA technique achieves higher sum rate with some level of fairness compared to static power allocation algorithms. In [26], a power control strategy was derived in a downlink OWC to maximize the sum rate of multiple users under the constraints of user-fairness and illumination. In [27], NOMA was implemented in a hybrid OWC/RF, where GRPA was used to distribute the power at a given user grouping. In [28], the performance of NOMA was enhanced in OWC through minimizing the transmit power per LED while achieving minimum data rate requirements for static users in the network. Interestingly, the formation of multiple groups in NOMA highly affects the power allocation techniques proposed in [25], [26], [27], [28]. Indeed, user grouping and power allocation in NOMA are defined as joint problems that must be solved to unlock the potential of NOMA for use in the next generation of wireless communications. In [16], a user grouping approach was proposed to form a number of groups in a multi-cell OWC network considering the locations of the users, and accordingly, the sum rate of the network is maximized through performing power allocation within each independent optical cell. In [29], cooperative NOMA was adopted in a RF-aided single optical cell network where user-grouping and power allocation problems are solved to maximize the sum rate of the users belonging to a certain group. In [30], a permutation-based genetic algorithm was proposed to optimize user pairings and enhance the performance of hybrid NOMA and orthogonal transmission in an OWC network. Despite the detailed work on NOMA in the literature of RF and OWC networks, this paper defines user-grouping, power allocation, user traffic demands, and overall system performance as joint problems that must be addressed to promote NOMA as a strong candidate in the emerging 6G OWC.

B. Main Contributions

In this paper, an OWC network is considered using arrays of IR lasers as optical APs operating within a limited range of transmit power according to eye safety regulations. This network is known for its high density, where a large number of APs is required to ensure uniform coverage for multiple users. Therefore, we propose a BIA outer precoder to coordinate the transmission among the optical APs with the guarantee of interference alignment for multiple groups of users formed according to the NOMA methodology. Note that, in [19], a semi-Blind interference management scheme was proposed by integrating BIA and NOMA in RF networks. To the best of our knowledge, this paper is the first to propose the integration of the two schemes in OWC. Moreover, in contrast to related works, including [19], a joint rate-maximization optimization problem is formulated to determine the optimal user grouping, efficiently distribute the power budget in the network, ensure the fulfillment of user traffic demands, and enhance overall system performance.

The main contributions are listed as follows

- An OWC system model is defined, which consists of a number of IR laser-based optical APs deployed to ensure uniform coverage for multiple-users. To overcome the limitations of NOMA, an outer precoder is designed for AP coordination by following the methodology of BIA. This precoder has also the ability to align interference among groups of users that can be formed under certain conditions. Therefore, the application of NOMA can be applied successfully within each group with relatively low noise, as a result of the effective management of both inter-cell and inter-group interference.
- A rate-maximization optimization problem is formulated subject to the constraints of unique elements within each group of users, low power consumption, and user traffic demand, to ensure high performance in NOMA-based transmission. By solving this optimization problem, the essential conditions mentioned above can be guaranteed. However, the optimization problem is defined as a max-min fractional program, which is complex and difficult to solve in practical scenarios. It is concave in nature and involves coupled optimization variables.
- To provide practical solutions, an RF-aided dynamic algorithm is designed to form multiple groups taking into consideration the locations of the users, where a portion of the resources of an RF system deployed for uplink transmission [23] is devoted for the strong and weak users to exchange binary variables and establish weak-strong user associations. Moreover, a dynamic power allocation algorithm is derived to maximize the sum rate of the users belonging to all the groups simultaneously, where different power levels are allocated to different groups based on the demands of the users within each group. The application of the proposed algorithm guarantees that each user experiences high quality of service regardless of its classification as weak or strong, and that the power budget of the network is consumed efficiently, which in turn maximizes the overall performance of the OWC

network.

The results demonstrate the high performance of the proposed dynamic application of NOMA in terms of data rate, energy efficiency, and fairness compared to BIA, traditional NOMA, and other benchmark schemes introduced according to the literature of NOMA. Moreover, the dynamic user-grouping and power allocation algorithms provide practical and significant solutions close to the optimal ones at low complexity.

Other parts of the paper are organized as follows. In Section II, the system model of the laser-based OWC network is described. The transmission based on NOMA, inter-group interference management and the sum rate of the network are derived in Section III. The optimization problem is formulated in Section IV. Section V presents the dynamic user-grouping and power allocation algorithms in detail. Finally, Section VI presents simulation results, and Section VII provides concluding remarks and future directions.

Notation. The mathematical notations invoked in this work are defined as follows. Bold upper case and lower case letters denote matrices and vectors, respectively. \mathbf{I}_M and $\mathbf{0}_M$ notations represent identity and zero matrices with $M \times M$ dimension, respectively. $\mathbf{0}_{M,N}$ denotes a $M \times N$ zero matrix. $[]^T$ and $[]^H$ indicate transpose and hermitian transpose operators, respectively. Finally, \mathbb{E} is the statistical expectation, and $\text{col}\{ \}$ is the column operator that stacks the vectors considered in a column.

II. SYSTEM MODEL

A downlink OWC network is considered as shown in Fig. 1. On the ceiling, a number of optical APs given by $L, l = \{1, \dots, L\}$, is deployed to provide wireless converge for K users, where $k = \{1, \dots, K\}$. In this work, all the L optical APs serve the K users simultaneously where the transmission is coordinated using BIA¹. Moreover, the users are classified as weak users denoted by K_w , where $i = \{1, \dots, K_w\}$, and as strong users denoted by K_s , where $j = \{1, \dots, K_s\}$ ². Each user is equipped with a reconfigurable optical detector of $M, m = \{1, \dots, M\}$, photodiodes to provide a wide field of view (FoV). This receiver also enables the user to switch its reception mode following a predefined pattern to provide linearly independent channel responses from L optical APs [20], [21]. In this context, the received signal at photodiode

¹The application of BIA over L optical APs results in full connectivity in the network [22]. Note that, our system model can be managed as a multi-cell scenario where an optimum user-AP association vector must be determined and inter-cell interference must be managed using various network topology approaches. These issues are not within the scope of this work. Nevertheless, the formulation of the optimization problem and the practical solutions derived in the paper can be easily extended to such multi-cell scenarios.

²The classification of the users is done according to the locations of the users, where the K_s strong users receive high power from all the optical APs due to their locations at the center of the room, i.e., $\text{dist}(l, i) \leq d_{\text{th}}, \forall l \in L, \forall i \in K_s$, where $\text{dist}(l, i)$ is the distance between user i and optical AP l and d_{th} is the threshold distance that results in a low received power. While the K_w weak users located at the edges receive weak power from the optical APs located at large distance [3]. Without loss of generality and to better understanding the derived schemes, a case of $K_s = K_w$ is considered in this work to form multiple groups each with a pair of users similarly to the majority of work in the NOMA literature, otherwise, $K_s \neq K_w$, virtual weak or strong users can be assumed with zero data rates.

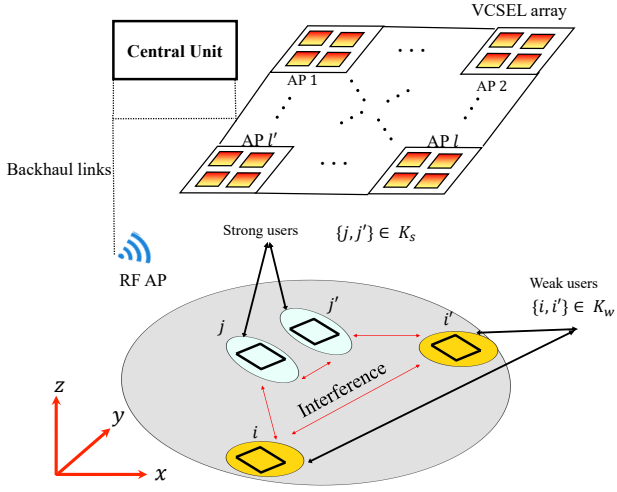


Fig. 1. An OWC network using IR lasers as transmitters serving multiple users.

m of a generic user $k \in K$ from L optical APs at time n can be expressed as

$$y^{[k]}[n] = f\mathbf{h}^{[k]}(m^{[k]}[n])^T \mathbf{x}[n] + z^{[k]}[n], \quad (1)$$

where f is the detector responsivity, $\mathbf{h}^{[k]}(m^{[k]}[n]) \in \mathbb{R}_+^{L \times 1}$, $m^{[k]}[n]$ is the channel state selected by photodiode m at time slot n , $\mathbf{x} = [x_1, x_2, \dots, x_L]^T \in \mathbb{R}_+^{L \times 1}$ is the transmitted signal where $x_l = \rho\sqrt{P_k}u_{k,l} + \rho \sum_{k' \neq k} \sqrt{P_{k'}}u_{k',l} + \rho I^{Dc}$ is the transmitted signal from AP l towards user k , where P_k is the power allocated to user k , $u_{k,l}$ is the desired message, I^{Dc} is the direct current that ensures the non-negativity of the signal and ρ is the electric to optical power conversion factor. Moreover, $\sum_{k' \neq k} \sqrt{P_{k'}}u_{k',l}$ is multi-user interference due to transmission to other users, and $z^{[k]}$ is real valued additive white Gaussian noise with zero mean and variance given by the sum of contributions from shot noise, thermal noise and the intensity noise of the laser. Finally, a WiFi AP is deployed for uplink transmission, where users send through it important information for performing various optimization problems with different objectives. All the APs in the network, optical and RF, are connected through a central unit (CU) that contains information on the distribution of users and their need of resources. It is worth mentioning that the need for CSI at the transmitters is subject to the use of the multiple access technique implemented to serve the active users in the network.

A. Optical transmitters

In this work, the VCSEL is used as a transmitter operating under eye safety regulations due to its high modulation speed, and each optical AP is defined as an array of $L_v \times L_v$ VCSELs to expand its confined coverage area. Interestingly, the VCSEL has a Gaussian beam profile, and parameters such as the beam waist W_0 , wavelength λ and beam travelling distance d_0 determine the power distribution of the VCSEL. In this context, the beam radius of the VCSEL at the receiving plane

located at distance d_0 is given by

$$W(d_0) = W_0 \left(1 + \left(\frac{d_0}{d_{Ra}} \right)^2 \right)^{1/2}, \quad (2)$$

where d_{Ra} is the Rayleigh range expressed as $d_{Ra} = \frac{\pi W_0^2 n}{\lambda}$, where n is the refractive index of the air, i.e., $n = 1$. Moreover, the spatial distribution of the intensity of the VCSEL over the transverse plane at the same distance d_0 is given by

$$I_{tr}(r, d_0) = \frac{2P_{tr}}{\pi W^2(d_0)} \exp \left(-\frac{2r^2}{W^2(d_0)} \right), \quad (3)$$

where r is the radial distance from the beam spot center and P_{tr} is the optical power per the beam. Note that, the detection area of each photodiode within the reconfigurable detector can be given by $A_m = \frac{A_{rec}}{M}$ with radius r_m , where A_{rec} is the whole detection area of the optical detector. Therefore, the optical power received at photodiode m of user k from a transmitter is given by

$$P_m = \int_0^{r_m} I_{tr}(r, d_0) 2\pi r dr = P_{tr} \left[1 - \exp \left(-\frac{2r_m^2}{W^2(d_0)} \right) \right], \quad (4)$$

considering a scenario of the photodiode m of user k is aligned with the transmitter. It is worth mentioning that each photodiode of the reconfigurable detector points to a distinct direction determined by elevation and azimuth angles, $\theta_{k,m}$ and $\alpha_{k,m}$, respectively, on the x-y plane. Thus, the normal vector of photodiode m of user k is

$$\hat{\mathbf{n}}_{k,m} = [\sin(\theta_{k,m}) \cos(\alpha_{k,m}), \sin(\theta_{k,m}) \sin(\alpha_{k,m}), \cos(\theta_{k,m})], \quad (5)$$

In different scenarios, the irradiance angle of the VCSEL in regard to user k is determined by $\phi_{tr}^{[k]} = \cos^{-1}(\frac{\hat{\mathbf{n}}_{tr} \cdot \mathbf{d}}{d})$, considering that $\mathbf{d} = \mathbf{P}_{tr} - \mathbf{P}_k$ is the distance vector given by the locations of the transmitter and user, \mathbf{P}_{tr} and \mathbf{P}_k , respectively, $d = \|\mathbf{d}\|$. At this point, $r = d \sin \phi_{tr}^{[k]}$, and d_0 is replaced by $d \cos \phi_{tr}^{[k]}$. Hence, the spatial distribution of the intensity of the VCSEL is defined as a function of the distance d and irradiance angle ϕ , i.e., $I_{tr}(d, \phi)$. In this context, the optical power received at photodiode m of user k from the VCSEL is given by

$$\begin{aligned} P_m &= I_{tr}(d, \phi) A_{pd} G_m \cos(\psi_{tr}^k(m)) \text{rect} \left(\frac{\psi_{tr}^k(m)}{\Psi_F} \right) \\ &= \frac{2 \cos(\psi_{tr}^k(m)) P_{tr} A_{pd} G_m}{\pi W^2(d \cos \phi_{tr}^{[k]})} \\ &\quad \exp \left(-\frac{2d^2 \sin^2 \phi_{tr}^{[k]}}{W^2(d \cos \phi_{tr}^{[k]})} \right) \text{rect} \left(\frac{\psi_{tr}^k(m)}{\Psi} \right), \end{aligned} \quad (6)$$

where A_{pd} and G_m is the detection area and gain of the photodiode, respectively. Moreover, $\psi_{tr}^k(m)$ is the angle between the normal vector $\hat{\mathbf{n}}_{k,m}$ and the distance vector \mathbf{d} , i.e., $\psi_{tr}^k(m) = \cos^{-1}(\frac{\hat{\mathbf{n}}_{k,m} \cdot \mathbf{d}}{d})$. Finally, Ψ_F is the field of view where $\text{rect} \left(\frac{\psi_{tr}^k(m)}{\Psi} \right) = 1$ if $0 \leq \psi_{tr}^k \leq \Psi_F$, or it equals zero otherwise.

TABLE I
TRANSMITTED SIGNAL FOR $L = 2, G = 2, K_g = \{i, j\}, K_{g'} = \{i', j'\}, g' \neq g$

	AP 1	AP 2
Time slot 1	$(u_{i,1} + u_{j,1}) + (u_{i',1} + u_{j',1})$	$(u_{i,2} + u_{j,2}) + (u_{i',2} + u_{j',2})$
Time slot 2	$u_{i,1} + u_{j,1}$	$u_{i,2} + u_{j,2}$
Time slot 3	$u_{i',1} + u_{j',1}$	$u_{i',2} + u_{j',2}$

B. Optical constraints

The use of VCSEL maximizes the communication speed of OWC due to its high modulation speed. However, the transmit optical power P_{tr} is limited for eye safety regulations. To calculate the maximum transmit power allowed per VCSEL $P_{tr,max}$, we define some notations as follows. The aperture diameter of the cornea is d_c , the exposure level of the cornea to the transmit power is E_e , the maximum exposure level is $E_{e,max}(t_e)$ as a function of the exposure duration t_e and the hazard distance is d_h at which eye injuries might happen. In this context, E_e at the hazard distance d_h can be calculated according to [2] as

$$\begin{aligned} E_e(d_h) &= \frac{1}{\pi(\frac{d_c}{2})^2} \int_0^{d_c/2} I(r, d_h) 2\pi r dr \\ &= \frac{1}{\pi(\frac{d_c}{2})^2} \int_0^{d_c/2} \frac{2P_{tr}}{\pi W^2(d_h)} \exp\left(-\frac{2r^2}{W^2(d_h)}\right) 2\pi r dr \\ &= \frac{P_{tr}}{\pi(\frac{d_c}{2})^2} \left(1 - \exp\left(-\frac{d_c^2}{2W^2(d_h)}\right)\right). \end{aligned} \quad (7)$$

Interestingly, the transmit power of the VCSLE is safe for the human eye if $E_e(d_h) \leq E_{e,max}(t_e)$, which means that the use of the VCSEL is safe regardless of the location of the user as in the most hazard location, the transmit power does not cause any harm to the human eye. Therefore, the maximum permissible power per beam is determined as

$$P_{tr,max} = \frac{\pi}{4} d_c^2 E_{e,max}(t_e) \left(1 - \exp\left(-\frac{d_c^2}{2W^2(d_h)}\right)\right)^{-1}. \quad (8)$$

More details on the calculation of $E_{e,max}(t_e)$ can be found in [2]. Given the eye safety regulations, the deriving current³ of the VCSEL I_v^{Dc} must be within a certain range of current $[I_L, I_H]$, ensuring that the VCSEL works in the linear region and that the corresponding deriving power $[P_L, P_H]$ guarantees eye safety. As a consequence, the peak amplitude of the modulated signal applied to the VCSEL, which might contain information intended to K generic users, is denoted by η_v , and it must be subject to the constraint $\eta_v \leq \min(I_v^{Dc} - I_L, I_H - I_v^{Dc})$. It is worth pointing out that each AP $l \in L$ is composed of $L_v \times L_v$ VCSELS, and therefore, $P_L \leq (P_l)/(L_v \times L_v) \leq P_H$, where P_l is the transmit power of the AP, ensuring that each VCSEL in the array of the AP emits the same power, i.e., $P_{tr,max} = (P_l)/(L_v \times L_v)$.

³A fixed DC-biasing is considered to focus our attention on optimizing power allocation among the messages intended to different users as adaptive signal scaling and DC biasing are critical in OWC that require independent studies [31].

III. NOMA-BASED TRANSMISSION

For an OWC network as shown in Fig. 1, we first design an outer precoder to coordinate transmission among L optical APs and to align interference across G groups formed based on channel gain differences, where each group $g \in G$ consists of $K_g = \{i, j\}$ users, classified as weak and strong users, i and j , respectively. Then, NOMA is considered within each group to manage intra-group interference, deriving the sum rate of the network.

A. Outer precoder design

An outer precoder is designed following the methodology of BIA proposed first in [18], [19].

Basically, BIA generates a transmission block over which alignment blocks are allocated to each group. Each alignment block is composed of L time slots, and the users of a certain group switch their reception modes over each of their alignment blocks following the same distinctive pattern to receive useful information. The construction of the BIA transmission block can be easily determined considering the number of APs and groups. In this case, it must contains $(L-1)^G + G(L-1)^{G-1}$ time slots divided into two sub-blocks, where sub-block 1 contains $(L-1)^G$ time slots and sub-block 2 contains $G(L-1)^{G-1}$ time slots. At this point, the number of alignment blocks allocated to each groups is $\zeta = \{1, \dots, (L-1)^{G-1}\}$ distributed over the transmission block with two conditions as follows

- **Ensuring coordination among L APs and the decodability of each symbol.** Each symbol transmitted to a certain group denoted by $\mathbf{u}_\zeta^{[g]}$ over the ζ -th alignment block must contains LK_g messages from L APs, i.e., $\mathbf{u}_\zeta^{[g]} = [u_{i,1} + u_{j,1}, \dots, u_{i,L} + u_{j,L}]^T$, where $u_{i,l}$ and $u_{j,l}$ are the messages transmitted by AP l to the weak and strong users forming group g , respectively. Thus, the users of each group must switch their reception modes among L modes, i.e., a predefined pattern, during the transmission of the ζ -th alignment block to achieve LK_g degrees of freedom (DoF) in $\mathbf{u}_\zeta^{[g]}$.
- **Inter-group interference alignment.** BIA can align the interference among multiple groups if the users $K_{g'}$ belonging to group $g' \in G, g' \neq g$ can measure the interference due to the transmission of the symbol $\mathbf{u}_\zeta^{[g]}$ over the ζ -th alignment block allocated to the K_g users belonging to group $g \in G$. It can be achieved by ensuring the reception modes of the $K_{g'}$ users remain the same while the K_g users change their reception modes to receive useful information transmitted over an alignment block. Given that, the interference can be aligned in

at least one dimension less compared to the desired information.

For illustrative purpose, a use case of $L = 2$ optical APs serving $G = 2$ groups, each group with $K_g = 2$ users, is shown in Table I, where the transmission block comprises $(2-1)^2 + 2(2-1)^{2-1}$ time slots, and $\zeta = (2-1)^{2-1}$ alignment blocks are allocated to each group. Note that, the K_g users are served over the time slots $\{1,2\}$ constituting the only one alignment block allocated to group g in this scenario, while the $K_{g'}$ users are served over the time slots $\{1,3\}$. Moreover, the users of group g use the third time slot to measure and subtract the interference received over the first time slot, while the users of group g' use the second time slot to measure and cancel the interference, due to the fact that orthogonal transmission is occurred over the second and third time slots. More mathematical details can be found in [18].

At this point, the transmitted signal for the general case can be expressed as

$$\mathbf{X} = \sum_{g=1}^G \mathbf{B}^{[g]} \left(\sqrt{P_w} \mathbf{u}_{i,T}^{[g]} + \sqrt{P_s} \mathbf{u}_{j,T}^{[g]} \right) + \rho I^{Dc} \times \mathbf{1}_{L \times 1}, \quad (9)$$

where P_w and P_s is the power allocated to the weak and strong users, respectively. Moreover, $\mathbf{X} = \text{col}\{\mathbf{x}(\kappa)\}_{\kappa=1}^{\mathcal{V}_L}$, where \mathcal{V}_L is the length of the transmission block designed according to the principles of BIA, $\mathbf{B}^{[g]}$ is the precoding matrix used by the K_g users belonging to group g , and $\mathbf{u}_{k,T}^{[g]} = \text{col}\left\{\mathbf{u}_{k,\zeta}^{[g]}\right\}_{\zeta=1}^{(L-1)^{G-1}}$, where $\mathbf{u}_{k,\zeta}^{[g]} = [u_{k,1}, \dots, u_{k,L}]^T$ contains the symbols transmitted to user k over each alignment block allocated to group g , $g \in G$, during the entire transmission block. Interestingly, once the transmission block is built and multiple alignment blocks are allocated to each group with the two conditions above, the precoding matrix $\mathbf{B}^{[g]}$ used by the users of the same group can be easily determined, where each alignment block ζ represents a column in the precoding matrix, stacking $L \times L$ identity matrices in the rows corresponding to the time slots that form each alignment block. After designing the precoding matrices from L APs to G groups, each user $i \in K_g$ is subject only to intra-group interference from its paired user $j \in K_g$, $K_g = \{i, j\}$, which can be canceled using NOMA as below.

B. NOMA

The received signal at weak user $i \in K_g$ can now be written as

$$\tilde{\mathbf{y}}_{g,i} = \rho f \left(\mathbf{H}^{[g,i]} \underbrace{\sqrt{P_w} \mathbf{u}_{i,\zeta}^{[g]} + \mathbf{H}^{[g,j]} \sqrt{P_s} \mathbf{u}_{j,\zeta}^{[g]}}_{\text{intra-group interference}} \right) + \tilde{\mathbf{z}}^{[g,i]}. \quad (10)$$

Note that, the received signal of the strong user $j \in K_g$ can be easily derived following the same fashion. It is worth pointing out that the power levels P_w and P_s must be determined carefully, $P_w > P_s$, giving each user the ability to decode its message [9]. Therefore, the achievable rate of a generic user k in a certain group g considering the use of the outer precoder and NOMA can be expressed as follows

$$R_{g,k} = b_{ab} \times \mathbb{E} \left[\log \det \left(\mathbf{I} + \gamma_{g,k} \mathbf{H}^{[g,k]} \mathbf{H}^{[g,k]H} \mathbf{R}_{\tilde{\mathbf{z}}}^{-1} \right) \right], \quad (11)$$

where $\gamma_{g,k}$ is the SINR of a generic user k taking into account the distinct features of the optical signal. It is given by $\gamma_{g,i} = \frac{c \rho^2 f^2 P_w}{c \rho^2 f^2 P_s + \sigma_z^2}$ and $\gamma_{g,j} = \frac{c \rho^2 f^2 P_s}{\sigma_z^2}$ for the weak and strong users, respectively, where $c = 1/2\pi e$ considering e as the Euler number. Moreover, b_{ab} is the ratio of alignment blocks allocated to each group due to the use of the outer precoder, it is given by $\frac{1}{L+G-1}$, and $\mathbf{R}_{\tilde{\mathbf{z}}}$ is the covariance matrix that results from subtracting the information sent to $G-1$ groups.

IV. SUM RATE MAXIMIZATION IN NOMA-BASED OWC

To enhance the performance of NOMA-based transmission in dense OWC networks, we formulate here an optimization problem that jointly optimizes user grouping and power allocation to maximize overall system performance while satisfying the traffic demands of all users, regardless of their classification as K_w or K_s .

Let us first define an association variable as $x^{[i,j]}$, $\{i, j\} \in K$, in order to pair each weak user i with a strong user j . Therefore, it equals to

$$x^{[i,j]} = \begin{cases} 1 & \text{, if weak user } i \text{ is paired with strong user } j, \\ 0 & \text{, otherwise.} \end{cases} \quad (12)$$

In this context, the sum rate of a pair of weak and strong users can be expressed as follows

$$R_{g,K_g}(P_w, P_s, x) = x^{[i,j]} \left(R_{g,i}(P_w, P_s) + R_{g,j}(P_s) \right), \quad (13)$$

where $K_g = \{i, j\}$ contains i and j users that form the potential group g . Note that, according to (12), $R_{g,K_g}(P_w, P_s, x) = 0$ if weak user i is not paired with strong user j , i.e., $x^{[i,j]} = 0$, otherwise, $x^{[i,j]} = 1$, and $R_{g,K_g}(P_w, P_s, x)$ can be determined easily from (11) after the application of BIA-NOMA for interference management, $g' \neq g$, $K_g \neq K_{g'}$, and $i \neq j$. An appropriate optimization problem can then be formulated to maximize the overall network performance as follow

$$\max_{\mathbf{p}} \left\{ \min_{\{i,j\} \in \mathbf{K}} \left\{ x^{[i,j]} \left(R_i(P_w, P_s) + R_j(P_s) \right) \right\} \right\} \quad (14a)$$

$$\text{s.t. } \sum_{i \in K_w} \sum_{j \in K_s} (P_w + P_s) \leq P_{\max}, \quad \forall i, j \in K \quad (14b)$$

$$\sum_{i \in K_w} x^{[i,j]} = 1, \quad \forall j \in K_s \quad (14c)$$

$$\sum_{j \in K_s} x^{[i,j]} = 1, \quad \forall i \in K_w \quad (14d)$$

$$P_s \leq P_s^T, \quad (14e)$$

$$P_w > P_s^T, \quad (14f)$$

$$R_{\min,k} \leq R_k(P) \leq R_{\max,k}, \quad \forall k \in K \quad (14g)$$

$$x^{[i,j]} \in \{0, 1\}, P_s \geq 0, \{K_w \cup K_s\} = K, \quad (14h)$$

Physically, the first constraint in (14) ensures that the power consumption in the network is equal or less than the maximum transmit power $P_{\max} = \sum_{l=1}^L P_l$, where P_l is determined according to the eye safety regulations as in the system model. The second and third constraints guarantee that every group contains a unique pair of weak and strong users, i.e., $\{i, j\} \in K_g, K_g \cap K_{g'} = \emptyset, g \neq g'$. Moreover, the fourth constraint in (14e) is imposed to limit the power allocated to the strong user such that the weak user manages the desired information of the strong user as noise while decoding its information [10]. The power constraint in (14f) guarantees that the weak user in a group receives higher power than the strong user, and therefore, users performing SIC can decode the information successfully in descending order. The constraints (14e) and (14f) also ease measuring the interference that results from the transmission to other groups [32]. Furthermore, the data rate constraint in (14g) ensures high quality of service for all the K users regardless of their classification as strong or weak users. It is worth mentioning that the data rate of each user goes towards the maximum value $R_{\max,k}$ if and only if other users receive their demands and the power consumption is less than P_{\max} . Otherwise, the data rate of each user goes towards the minimum data rate $R_{\min,k}$, ensuring that all the users evenly experience high quality of service. The last constraint gives the fact that the strong user receives a non-zero power and the feasible region of the optimization problem formulated based on the principles of NOMA.

The optimization problem in (14) is classified as a max-min fractional program that has high complexity with a concave objective function [33], [34]. Moreover, the coupling of power allocation and user grouping makes the optimization problem infeasible to solve especially in scenarios that require practical solutions with low computational time. Therefore, we propose to divide the main problem into two sub-problems that can be solved separately to reduce the complexity. In particular, weak and strong users can form multiple groups based on the distance rather than the achievable data rates, where it was demonstrated in [10] that the application of NOMA in wireless communications among two users becomes more successful if those users considerably differ in their channel gains. Then, power allocation can be performed among the groups formed earlier to maximize the overall sum rate of the NOMA-based OWC network, while ensuring that the users in each group receive their traffic demands. It is worth mentioning that the reduction in complexity might come at the cost of providing sub-optimal solutions.

V. DYNAMIC USER GROUPING AND POWER ALLOCATION ALGORITHMS FOR NOMA

We design an RF-aided dynamic algorithm to perform user grouping based on the distance between users that can potentially be grouped, ensuring a high channel gain difference between them. Subsequently, a closed-form optimization problem is formulated for power allocation among the formed groups. This power allocation problem can be solved using an efficient dynamic algorithm that ensures fulfilling the traffic demands of the users belonging to all the group, which in

turn minimizes power waste and maximizes the total sum rate of the network. In the following, these dynamic algorithms for user grouping and power allocation are reported in detail.

A. Dynamic user-grouping algorithm for NOMA

A distance-based weight denoted as $w(\text{dist})$ is considered to determine optimal weak user-strong user combinations. It is worth mentioning that in the system model considered, an RF system is deployed to provide uplink transmission in the network. In this context, some of the RF system resources $(1 - e_{\text{rf}})$, where e_{rf} is a real value between 0 and 1, are dedicated for the users to exchange binary variables among them. In [10], it was reported that NOMA provides a high sum rate in a group, whose users, weak and strong users, differ considerably in the channel gain. Given that, the users in the network can be considered as vertices distributed on the receiving plane. Then, each strong vertex sends a binary variable through the RF system to all the weak vertices to establish distance-based weight edges. For instance, the distance-based weight of an edge $w(\text{dist})(j \rightarrow i)$ between weak user i and strong user j can be given as follows

$$w(\text{dist}(j \rightarrow i)) = \sqrt{(x_i - x_j)^2 + (y_i - y_j)^2}, \quad (15)$$

where (x_i, y_i) and (x_j, y_j) are the coordinates of weak user i and strong user j , respectively. Note that, the distance-based weight of edge $j \rightarrow i$ in (15) increases with the distance between weak user $i \in K_w$ and strong user $j \in K_s$. Interestingly, the channel gain of the user is dictated by its location from the optical transmitters. Therefore, the strong users are characterized by their high channel gains due to their locations at the center of the receiving plane, while the weak users located away from the optical transmitters receive a low channel gain. In this context, weak user $i \in K_w$ must be paired with strong user $j \in K_s$ if and only if the edge $j \rightarrow i$ has the highest weight compared to other edges between strong user j and other weak users, $j \rightarrow i'$, where $i' \neq i$, and $i' \in K_w$. That is, each group can be formed as follows

$$g^*(i, j) = \arg \max_x \sum_{i \in K_w} \sum_{j \in K_s} x^{[i, j]} w(\text{dist}(j \rightarrow i)), \quad (16)$$

where $\sum_{j \in K_s} x^{[i, j]} = 1, \forall i \in K_w$, $\sum_{i \in K_w} x^{[i, j]} = 1, \forall j \in K_s$ and $x^{[i, j]} \in \{0, 1\}$, $K_w \cup K_s = K$, ensuring that each group g is composed of unique elements according to the constraints in (14). This optimization problem can be solved through simply searching for optimal weak user-strong user combinations, forming G groups, each group with $K_g = \{i, j\}$ distinct users, i.e.,

$$\begin{aligned} K_g &= i \cup j, K_{g'} = i' \cup j', K_g \cap K_{g'} = \emptyset, \\ (i &\neq i', j \neq j', g \neq g'), \{i, i'\} \in K_w, \{j, j'\} \in K_s, \\ \{g, g'\} &\in G, K_w \cup K_s = K. \end{aligned} \quad (17)$$

B. Power allocation

Once each weak user is paired with a strong user, the problem in hand is to perform power allocation among multiple groups formed at the earlier stage and under the constraints

of power budget and high quality of service. Therefore, the optimization problem in (14) can be rewritten as follows

$$\max_{\mathbf{P}} \left\{ \min_{g \in G} R_{g, K_g}(P_w, P_s) \right\} \quad (18a)$$

$$\text{s.t. } \sum_{i \in K_w} \sum_{j \in K_s} (P_w + P_s) \leq P_{\max}, \quad \forall i, j \in K \quad (18b)$$

$$P_s \leq P_s^T, \quad (18c)$$

$$P_w > P_s^T, \quad (18d)$$

$$R_{\min, k} \leq R_{g, k}(P) \leq R_{\max, k}, \quad \forall k \in K \quad (18e)$$

$$P_s \geq 0, \{K_w \cup K_s\} = K, g \in G, \quad (18f)$$

where $R_{g, K_g}(P_w, P_s)$ is the sum rate of the group comprising K_g users. To solve (18), we introduce a dynamic power allocation algorithm to provide significant sum rate maximization at lower cost compared to solving the complex optimization problem in (14). It is a practical algorithm that runs for the K_g users of each group to achieve the highest sum rates while ensuring that the users belonging to the other groups experience high data rates. In particular, the power constraint in (18) is divided by a number T , where $t = \{1, \dots, t, \dots, T\}$, to have levels of the power constraint. That is

$$P_{\max, t} = \left\{ \frac{tP_{\max}}{T} : t = \{1, 2, \dots, T\} \right\}. \quad (19)$$

Assuming at the beginning of the proposed algorithm that no user is served, and therefore the sum rate of the network $R_{n, G}(P_w, P_s)$ under the power constraint $P_{\max, t}$ can be expressed as follows

$$R_{n, G}(P_w, P_s) = 0, \text{s.t. } \sum_{i \in K_w} \sum_{j \in K_s} (P_w + P_s) \leq P_{\max, t}, \\ P_w = 0, P_s = 0, \forall g \in G, \forall K_g \in K, \forall t \in T, \quad (20)$$

Subsequently, the sum rate of the K_g users belonging to group g selected randomly in this stage must be determined at each power constraint with the condition of dedicating power for the other users belonging to the groups considered prior to group g . Therefore, under the power constraint $P_{\max, t}$, the optimization problem can be simply expressed as

$$\max_{\mathbf{P}} R_{g, K_g}(P_w, P_s) \quad (21a)$$

$$\text{s.t. } (P_w + P_s) \leq P_{\max, t}, \quad \forall t \in T \quad (21b)$$

$$P_s \leq P_s^T, \quad (21c)$$

$$P_w > P_s^T, \quad (21d)$$

$$R_{\min, k} \leq R_{g, k}(P) \leq R_{\max, k}, \quad \forall k \in K_g \quad (21e)$$

$$P_s \geq 0, \{i, j\} \in K_g, K_g \in K, g \in G. \quad (21f)$$

Note that, the achievable data rate of the weak user is a function of the power values allocated to the strong and weak users due to the interference term in (11). Given that, the assumption of serving the strong users at the highest possible power P_s^T is considered, and an upper bound of multi-user interference received at the weak user can be derived, which means that the interference is a constant [32].

Proposition: A parametric approach at a given parameter

[33] can be invoked to solve the optimization problem in (21). That is, the objective function can be transformed into

$$\mathcal{L} = \max_{\mathbf{P}} \left\{ R_{g, K_g}(P_w, P_s) - \theta \right\}, \quad (22)$$

where $\theta = \xi_g(P_w + P_s)$, considering that ξ_g is a non-negative parameter given by $R_{g, K_g}(P_w, P_s)/P_g^T$, where P_g^T is the total power consumed by the pair of users, $\{i, j\} \in K_g$.

Proof. See the Appendix \square

Interestingly, if each of the K_g users receive the maximum data rate $R_{\max, k}$ and the power consumption $P_{\max, g} > P_{\max, t}$, it means that the $(K' - K_g)$ users, where K' is the number of the users belonging to the groups considered until this stage, receive 0 power under the power constraint $P_{\max, t}$. Therefore, the data rate of each of the K_g users must decrease towards the minimum data rate $R_{\min, k}$, such that the power constraint $P_{\max, t}$ can be enough to support at least K_g users. Otherwise, if the power consumption $P_{\max, g}$ is still higher than $P_{\max, t}$, then, there is no feasible solution for the network to support (K') users under that power constraint. Therefor, the power is slightly relaxed to $P_{\max, t+1}$, and the same procedure is followed considering the new power constraint.

Let us consider the other scenario in which the power consumption $P_{\max, g} \leq P_{\max, t}$, and the K_g users receive data rates within the specified range $R_{\min, k} \leq R_{g, k}(P) \leq R_{\max, k}$. In this case, the fractional power resulting from $(P_{\max, t} - P_{\max, g})$ is used to support $(K' - K_g)$ users, each K_g belongs to a certain group. Therefore, the overall maximum sum rate of the network $R_{n, G'}(P_{\max, t})$, where G' is the number of the total groups considered until this stage, under the power constraint $P_{\max, t}$ can be determined according to a recursive equation as follows

$$R_{n, G'}(P_{\max, t}) = \max_p \left\{ R_{n, K' - K_g}(\lfloor P_{\max, t} - P_{\max, g} \rfloor) + R_{g, i}(P_w^*, P_s^*) + R_{g, j}(P_s^*), \right. \\ \left. \{i, j\} \in K_g, (P_{\max, t} - P_{\max, g}) \geq 0 \right\}, \quad (23)$$

where $R_{n, K' - K_g}(\lfloor P_{\max, t} - P_{\max, g} \rfloor)$ is the maximum sum rate of the network for $(G' - 1)$ groups by allocating the remaining power $(P_{\max, t} - P_{\max, g})$. Note that, the floor operation $\lfloor \cdot \rfloor$ is used to obtain a round power value due to the fact that the remaining power $(P_{\max, t} - P_{\max, g})$ might not equal to any of the power levels, and therefore, the nearest lower level can be considered resulting in the fact that $R_{n, K' - K_g}(\lfloor P_{\max, t} - P_{\max, g} \rfloor)$ is one of the solutions in the previous stage. It is worth mentioning that the procedure explained above is repeated for all the levels of the power constraints until the original power constraint P_{\max} in (18) is reached, and that the sum rate of the network is determined according to equation (24).

Once the procedure above is applied for G groups, i.e., $G' = G$ and $K' = K$, the maximum sum rates of the groups are collected and stored in a set denoted by $\mathcal{R}_{n, G} \in \mathbb{R}^{(G \times T)}$ in which the sum rate of $K, k = \{1, \dots, K\}$, users arranged in $G, g = \{1, \dots, G\}$, groups for each power constraint

$P_{max,t}, t = \{1, \dots, T\}$, e.g., $R_{n,K}(P_{max,t})$, can be found. Note that, the maximum sum rates of the G groups containing K users are determined after specifying target data rates within the range $R_{min,k} \leq R_{g,k}(P) \leq R_{max,k}$, for the weak and strong users, $\{i, j\} \in K_g$, belonging to each group g , which can be reached according to a certain power allocation strategy under each power constraint. Therefore, a set denoted by $\mathcal{T}_{n,K} \in \mathbb{R}^{(K \times T)}$ is assumed to host all the target data rates for the K users in the network. Moreover, a set denoted by $\mathcal{P}_{n,K} \in \mathbb{R}^{(K \times T)}$ is assumed to host the potential power values for the K users in the network. Note that, the results in the set of the maximum sum rates $\mathcal{R}_{n,G} \in \mathbb{R}^{(G \times T)}$ are associated with the corresponding sets $\mathcal{T}_{n,K}$ and $\mathcal{P}_{n,K}$ for user-demands and power allocation, respectively. Given that, each column in the set $\mathcal{T}_{n,K}$ is $[\mathcal{T}_{n,K}]_{(:,t)}$, as well as a column in the set $\mathcal{P}_{n,K}$ is expressed as $[\mathcal{P}_{n,K}]_{(:,t)}$.

Finally after arranging the potential solutions for reaching the maximum possible sum rate in the network in three different sets considering the group formation for the NOMA application, an optimization problem is formulated to select the most effective solution from these sets as follows

$$\max_{G,t} \sum_{g \in G} R_{g,K_g}(P_w, P_s) \quad (25a)$$

$$\text{s.t. } \sum_{k \in K} [\mathcal{P}_{n,K}]_{(k,t)} \leq P_{max} \quad \forall t \in T \quad (25b)$$

$$R_{min,n} \leq \sum_{k \in K} [\mathcal{T}_{n,K}]_{(k,t)} \leq R_{max,n}, \quad \forall t \in T \quad (25c)$$

$$K_g \in K, t \in T, g \in G, \quad (25d)$$

where $R_{min,n}$ and $R_{max,n}$ are the minimum and maximum sum rates required in the network, respectively. Interesting, this range of data rate is defined in the network to guarantee that dividing the power constraint into different levels as in (19) does not affect the overall energy efficiency of the network, while the power constraint is slightly relaxed to the maximum permissible power P_{max} to consume in the network.

The following procedure is applied to solve the optimization problem in (25):

- All the maximum sum rate solutions in the set $\mathcal{R}_{n,G} \in \mathbb{R}^{(G \times T)}$ are considered to solve the optimization problem in (25), except the values that violate the constraints in (25c) and (25b), which are set to $-\infty$. Similarly, the corresponding values of target data rates and power allocation in the sets $\mathcal{T}_{n,K}$ and $\mathcal{P}_{n,K}$ are set to 0, if and only if they do not comply with the constraints of the optimization problem in (25).

- To search for the maximum sum rate, if $R_{n,G}(P_{max,t}) = R_{n,G'}(P_{max,t})$, while $G' < G$, then our algorithm chooses $R_{n,G}(P_{max,t})$ in order to serve more groups, i.e., more users, under the same power constraint, which in turn ensures higher spectral efficiency. On the other hand, if $R_{n,G}(P_{max,t}) = R_{n,G}(P_{max,t'})$, while $P_{max,t} < P_{max,t'}$, then, the proposed algorithm chooses $R_{n,G}(P_{max,t})$ due to the fact that the same number of users can be served at lower power consumption, which highly maximizes the energy efficiency of the network while considering the trade-offs with the spectral efficiency. In the context, the optimization problem to choose the optimum values of G^* and t^* can be expressed as $\{G^*, t^*\} = \arg \max_{G,t} \sum_{g \in G} R_{g,K_g}(P_w, P_s)$, giving higher priority for the total number of groups over the power consumption. Note that, imposing the power constraint in (25b) guarantees that serving the users at high power is still under the allowed power consumption in the network.

- The maximum sum rate $R_{n,G^*}(P_{max,t^*})$ is achieved according to the target data rates of the K users in $[\mathcal{T}_{n,K}]_{(:,t^*)}$ using the power allocation strategy in $[\mathcal{P}_{n,K}]_{(:,t^*)}$ under the power constraint P_{max,t^*} . In other words, the weak and strong users, $\{i, j\} \in K_g$, belonging to each group g receive their optimum power values P_w^* and P_s^* , respectively, based on the power allocation $[\mathcal{P}_{n,K}]_{(:,t^*)}$, which already guarantees that the other $(K - K_g)$ users belonging to other groups, $g' \neq g$, receive enough power to fulfill their demands determined based on $[\mathcal{T}_{n,K}]_{(:,t^*)}$.

To conclude, the original optimization problem in (14) can be solved by applying the proposed dynamic power allocation algorithm after the formation of multiple groups considering the principles of NOMA. In particular, the solution of the optimization problem in (25) is global in the network and close to the optimum solution if the above steps are applied successfully due to the fact that the sets, $\mathcal{R}_{n,G}$, $\mathcal{T}_{n,K}$ and $\mathcal{P}_{n,K}$ are generated in accordance to the original constraints of the main optimization problem.

VI. SIMULATION RESULTS

An indoor environment with $8\text{m} \times 8\text{m} \times 3\text{m}$ dimensions is considered to evaluate the performance of the dynamic application for NOMA in OWC networks. On the ceiling, $L = 4 \times 4$ optical APs are deployed to ensure coverage for $K = 20$ users classified as $K_w = 10$ and $K_s = 10$ weak and strong users, respectively. According to [2], the angle

$$R_{n,G'}(P_{max,t}) = \begin{cases} -\infty, & P_{max,g} > P_{max,t}, g \in G, 1 \leq t \leq T, 1 \leq G' \leq G \\ R_{g,i}(P_w^*, P_s^*) + R_{g,j}(P_s^*), & P_{max,t} - P_{max,g} = 0, \{i, j\} \in K_g, 1 \leq t \leq T, 1 \leq G' \leq G \\ \max_p \left\{ R_{n,K'-K_g}(\lfloor P_{max,t} - P_{max,g} \rfloor) + R_{g,i}(P_w^*, P_s^*) + R_{g,j}(P_s^*) \right\}, & P_{max,t} - P_{max,g} > 0, 1 \leq t \leq T, 1 \leq K' \leq K, 1 \leq G' \leq G. \end{cases} \quad (24)$$

TABLE II
SIMULATION PARAMETERS

Parameter	Value
Transmitter Bandwidth	1.5 GHz
Spectral response range	950-1700 nm
Laser wavelength	1550 nm
Laser beam waist	8 μ m
Physical area of the photodiode	15 mm ²
Receiver FOV	60 deg
Detector responsivity	0.9 A/W
Gain of optical filter	1.0
Laser noise	-155 dB/Hz

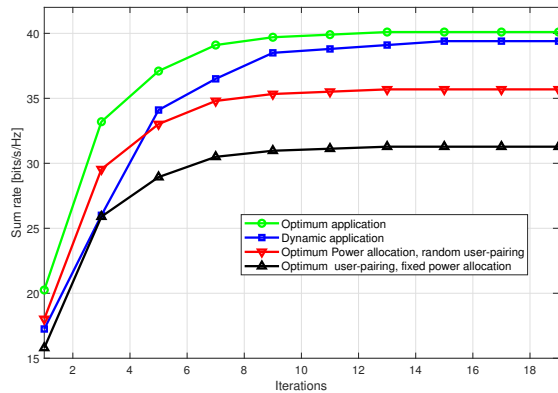


Fig. 2. Sum rate versus a set of iterations for various optimization problems.

for full width at half maximum intensity points Θ_F , which affects the divergence angle Θ_D and beam waist W_0 , is a vital parameter in VCSEL that must be considered to calculate the transmit optical power that is safe for the human eye, where $\Theta_D = \Theta_F / \sqrt{2 \ln(2)}$, and $W_0 = \frac{\lambda}{\pi \Theta_D}$. In this context, 60 mW is set as the maximum transmit optical power per beam for $\Theta_F = 4^\circ$. All the other parameters are in Table II. For comparison, two baseline schemes are proposed as counterpart schemes, which work in a similar fashion to the majority of work in the NOMA literature. In Baseline 1, the BIA outer precoder is used to manage interference among multiple groups formed using the proposed dynamic user-grouping algorithm, while a fixed power $P_{\max,g} = \frac{P_{\max}}{G}$ is allocated to each group in order to maximize the sum rate of each group independently through solving the optimization problem in (21), where $P_{\max,t}$ is replaced by $P_{\max,g}$. In Baseline 2, the proposed dynamic application is used for NOMA, and the bandwidth is divided by the number of groups G to allocate an exclusive resource block for each group to avoid inter-group interference rather than determining the precoding matrices of the groups, $\mathbf{B} = [\mathbf{B}^{[1]}, \dots, \mathbf{B}^{[g]}, \dots, \mathbf{B}^{[G]}] \in \mathbb{R}_+^{L \times G}$, following the methodology of BIA.

Fig. 2 shows the convergence of the proposed algorithms to the optimal solution against a set of iterations. It is shown that the dynamic application of NOMA provides significant solutions close to the optimal one, which is obtained by solving the two subproblems via exhaustive search in an alternating fashion. The proposed dynamic approach has low complexity that equals to $\mathcal{O}(TIK_gG)$, where I is the total

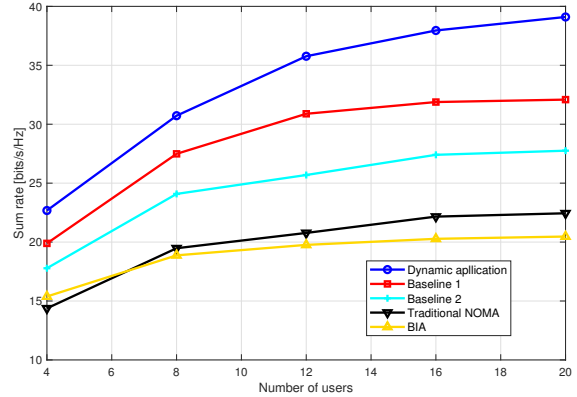


Fig. 3. Sum rate versus different numbers of users for the proposed NOMA-based dynamic algorithm.

number of iterations needed to maximize the sum rate of the K_g belonging to a certain group g , plus $\mathcal{O}(T)$ of solving the optimization problem in (25). The figure also shows that the optimization of power allocation with random user-pairing penalizes the sum rate of the network compared to the optimal and sub-optimal solutions. Furthermore, the formation of optimum groups cannot exploit the potential of NOMA if fixed power allocation is considered. Note that, in the context of our work, power allocation is crucial for NOMA due to the fact that the optimization problem in (14) is formulated to maximize the total sum rate of the network and fulfill the traffic demands of the users in each group. From now on, the proposed dynamic application of NOMA is considered for the rest of the results due to its optimality at low complexity.

Fig. 3 shows the sum rate of the network versus different numbers of users using the proposed dynamic application of NOMA compared to other benchmark schemes. It can be seen that the sum rate of the network increases with the number of users regardless of the scheme considered as the users differ their channel gains according to their locations from the optical APs. However, the sum rate increases slightly with any number of users beyond 15 due to the lack of the resources. The dynamic application of NOMA is superior compared to Baselines 1 and 2 due to the use of the outer precoder to avoid inter-group interference, rather than allocating orthogonal frequency or time slot to each group as in Baseline 2, and the use of the dynamic power allocation, which iterates over the groups to determine the optimum power values allocated to all the users in the network, compared to maximizing the sum rate of each group independently as in Baseline 1. It is worth mentioning that the conventional NOMA scheme provides low sum rates since the formation of multiple groups is obtained based on the channel gain difference between the weak and strong users, while fixed power is allocated to each user without considering the demands of the users and the maximization of the sum rate in the network. Moreover, BIA achieves the lowest sum rates compared to NOMA schemes as its performance is subject to a large transmission block and high noise in high density OWC networks [18], [22].

Blockage of direct optical links is a severe issue in OWC. Hence, the performance of the proposed scheme is evaluated in Fig. 4 against blockage probability. It can be seen that the

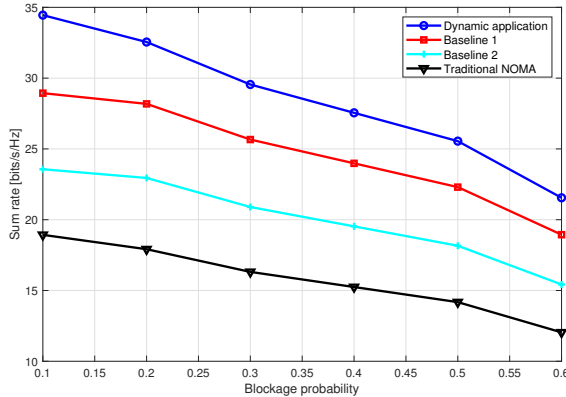


Fig. 4. Sum rate versus blockage probability for different NOMA schemes.

sum rate of the network decreases as the blockage probability increases from 0.1 to 0.6 as some of the weak users might be blocked from receiving service from any optical APs, and some of the strong users might be classified as weak users. However, the proposed dynamic application of NOMA achieves high performance compared to the benchmark schemes due to the fact that the power allocated to each user is determined according to its classification and its requirements of resources sent through RF uplink transmission to guarantee high quality of service. Similarly, in Baselines 1 and 2, the power is determined according to the demands of the users. However, the power devoted to each group is limited in Baseline 1, and each group is served over an orthogonal transmission block in Baseline 2. It is worth pointing out that at high blockage probabilities beyond 0.6, uncovered users can experience handover to the RF network in accordance to optimization problems with load balancing objective functions [23]. However, it is not in the scope of the paper.

Fig. 5 shows the performance of the proposed dynamic application of NOMA against SNR. It can be seen that the proposed dynamic algorithm provides high sum rates at different SNR values due to the use of power in a more effective way, satisfying the demands of the users. In other words, if a certain user experiences low SNR due to its location, our algorithm can still satisfy its requirements if the power budget is not fully consumed. Baseline 1 shows better performance compared to Baseline 2 and the conventional NOMA as the SNR increases. It is because of the implementation of the outer precoder for inter-group interference and optimizing the sum rate of the users belonging to each group. However, Baseline 1 uses fixed power allocation strategy among the groups formed in the network, which means that if the users of a certain group demand more power to experience high quality of service, Baseline 1 might fail to balance the load in the network causing power loss.

In Fig. 6, the sum rate of the network is depicted against W_0 ranging from 4–8 μm , which determines the AP coverage area and the transmit power. It is worth mentioning that any values beyond 8 μm , the optical power per transmitter must be recalculated accordingly. It can be seen that the sum rate of the network increases with the beam waist due to the fact that as W_0 increases, the illuminated area of each transmitter becomes

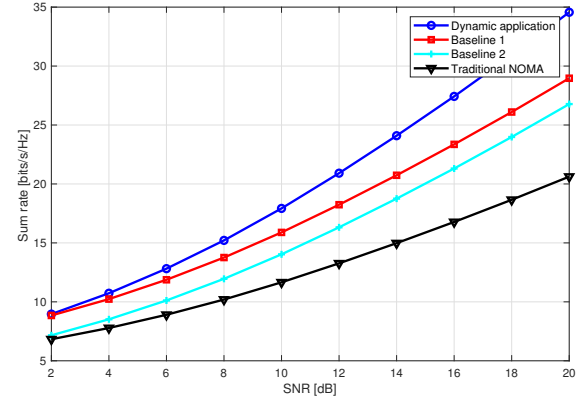
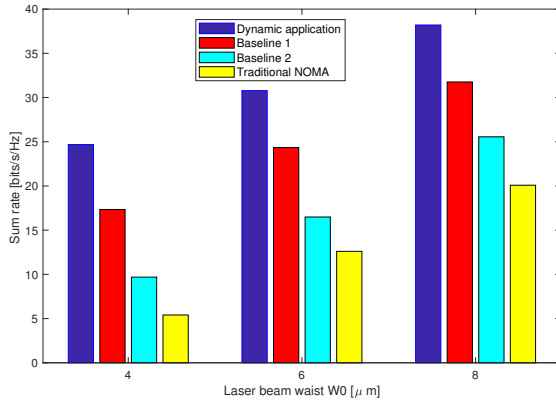
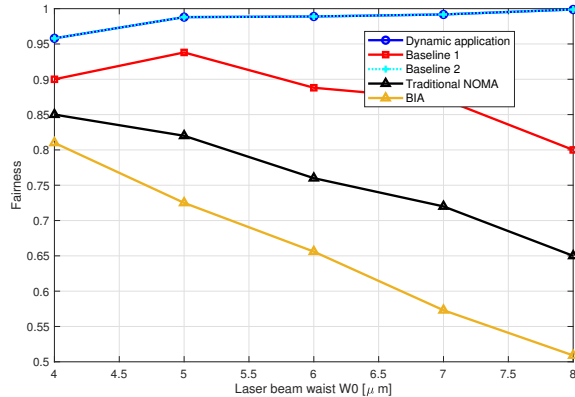


Fig. 5. Sum rate versus SNR for different NOMA-based schemes.

more confined focusing more power towards the users located at the center of the room, i.e., the strong users, while the weak users located at the edges of the optical cells receive low power. However, the proposed dynamic application of NOMA considers the conditions of each user and allocates power that satisfies its demands. The figure also shows the superiority of the proposed dynamic algorithm compared to the benchmark schemes. On the other hand, Fig. 7 shows one of the important metrics in NOMA against the beam waist, which is fairness using Jain's fairness index as NOMA considers the channel gain of the user in power allocation. Interestingly, the fairness of the proposed scheme increases with the increase of the beam waist. It is because of, at 4 μm , the channel gains of the strong users are less compared to the case of 8 μm . Note that, in the formulated optimization problem, the maximum power allocated to each strong user must be $P_s \leq P_s^T$, which might not be enough for the strong user at 4 μm beam waist. In contrast, the weak users receive their demands in all the scenarios considered, i.e., $P_w > P_s^T$. It is worth pointing out that, Baseline 2 achieves high fairness similar to the proposed dynamic application due to the implementation of the dynamic power allocation algorithm. While, in Baseline 1, the fairness increases with the beam waist, and it starts to decrease with any value beyond 5 μm . It can be interpreted that when the beam waist increases, the weak user belonging to each group demands more power, and the power budget of each group is limited to $P_{\max,g}$. Conventional NOMA and BIA result in poorer fairness compared to the proposed scheme, as NOMA ignores user demands and BIA allocates power equally regardless of channel gains.

In Fig. 8, the energy efficiency of the network is shown against the transmit power per beam to further examine the proposed dynamic use of NOMA in OWC networks. It can be seen that the energy efficiency decreases as the power increases due to power consumption. However, the dynamic application of NOMA is more efficient compared to Baselines 1 and 2 as the algorithm iterates over the groups formed to maximize the overall sum rate of the network. Interestingly, Baseline 2 overcomes Baseline 1 at low transmit power due to the implementation of the dynamic power allocation, while Baseline 1 achieves lower energy efficiency compared to the proposed scheme due to the fact that each group receives

Fig. 6. Sum rate versus W_0 for different NOMA schemes.Fig. 7. Fairness of the proposed dynamic algorithm versus W_0 .

fixed power, and users belonging to different groups might differ in their demands, and therefore, some users might not use the full power allocated to their corresponding group, and other users need more power than $P_{\max,g}$. The conventional NOMA scheme achieves low energy efficiency compared to the rest of the schemes as power allocation is performed without considering the needs of the users.

VII. CONCLUSIONS

In this paper, a dynamic application for NOMA is proposed in a laser-based OWC network to provide high quality of service for multiple users arranged into groups. We first define the system model consisting of multiple optical APs, where each AP is an array of VCSELs, derive the optical channel to determine user connectivity, and introduce optical constraints to ensure adherence to eye safety regulations. Then, a BIA outer precoder is designed for AP coordination and inter-group interference management, enabling the application of NOMA in each group. Finally, an optimization problem is formulated to maximize the sum rate of the network though jointly optimizing weak-strong user combinations and power allocation, while fulfilling user traffic demands. The main optimization problem is a max-min fractional program, which is difficult to solve in practice. Therefore, two dynamic algorithms are designed to solve the user grouping problem and power allocation separately with the guarantee of convergence to the optimal solution. The results show the superiority of the proposed dynamic application of NOMA in terms of data rate, energy efficiency, and fairness compared to counterpart

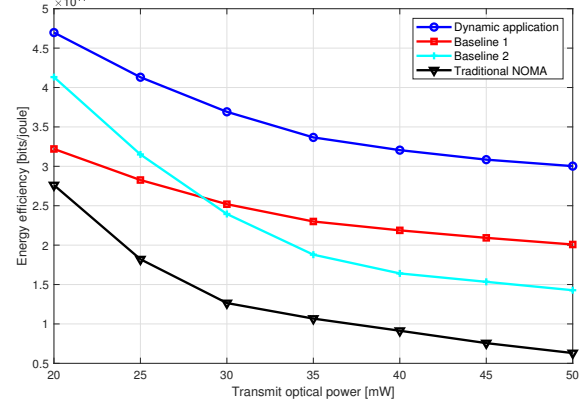


Fig. 8. Energy efficiency of the proposed NOMA scheme compared to the counterpart schemes for a range of transmit optical power per transmitter.

schemes introduced according to the literature of NOMA. For future work, BIA outer precoders have limitations in terms of transmission block size and inherent noise, and therefore, new precoder structures can be determined by formulating rate-maximization and OWC-RF load balancing problems under the constraints of BIA and NOMA. Additionally, machine learning algorithms can be implemented to provide solutions to these complex problems with real-time adaptability.

APPENDIX

By finding a root of equation $\mathcal{L}(\xi_g) = 0$ using a Dinkelbach-based algorithm [34] under the constraints of NOMA in (21), the sum rate of group g can be maximized. The Lagrangian function of (22) for weak user $i \in K_g$ belonging to group g under the constraints in (21) can be expressed as

$$\begin{aligned} \mathcal{L}_i = & R_{g,i}(P_w, P_s^T) - \xi_g(P_w + P_s^T) + \alpha_g(P_{\max,g} - (P_w + P_s^T)) \\ & + \mu_{g,i}(P_w - P_s^T) + \lambda_{\max,i}(R_{\max,k} - R_{g,i}(P_w, P_s^T)) \\ & + \nu_{\min,i}(R_{g,i}(P_w, P_s^T) - R_{\min,k}), \end{aligned} \quad (26)$$

where α_g , $\mu_{g,i}$, $\lambda_{\max,i}$ and $\nu_{\min,i}$ are Lagrangian multipliers defined to determine the power allocated to the weak user according to the constraints in (21b), (21d) and (21e), respectively. Using the Karush-Kuhn-Tucker (KKT) conditions [21], [34], the partial derivative $\frac{\partial \mathcal{L}_i}{\partial P_w} = 0$, i.e.,

$$\frac{\partial \mathcal{L}_i}{\partial P_w} = (\nu_{\min,i} - \lambda_{\max,i} + 1) \frac{R_{g,i}(P_w, P_s^T)}{\partial P_w} - \xi_g + \alpha_g - \mu_{g,i} = 0. \quad (27)$$

At given values for ξ_g , α_g , $\mu_{g,i}$, $\lambda_{\max,i}$ and $\nu_{\min,i}$, the optimum power P_w^* for the weak user, $i \in K_g$, can be found, and equation (26) can be updated considering that optimum power. Subsequently, the dual problem can be solved using the gradient projection method, and the Lagrangian multipliers related to power allocation and user demands are updated as follows

$$\mu_{g,i}(\tau) = [\mu_{g,i}(\tau - 1) - \epsilon_1(\tau - 1)(P_w(\tau - 1) - P_s^T)]^+, \quad (28)$$

$$\alpha_g(\tau) = \left[\alpha_g(\tau - 1) - \epsilon_2(\tau - 1) \left(P_{\max,g} - (P_w(\tau - 1) + P_s^T) \right) \right]^+, \quad (29)$$

$$\lambda_{\max,i}(\tau) = \left[\lambda_{\max,i}(\tau-1) - \epsilon_3(\tau-1) \right. \\ \left. \left(R_{\max,k} - R_{g,i}(P_w, P_s^T)(\tau-1) \right) \right]^+, \quad (30)$$

$$\nu_{\min,i}(\tau) = \left[\nu_{\min,i}(\tau-1) - \epsilon_4(\tau-1) \right. \\ \left. \left(R_{g,i}(P_w, P_s^T)(\tau-1) - R_{\min,k} \right) \right]^+, \quad (31)$$

where τ denotes the iteration of the gradient algorithm, and $[.]^+$ is a projection on the positive orthant taking into consideration that $\mu_{g,i}, \alpha_g, \lambda_{\max,i}, \nu_{\min,i} \geq 0$. Moreover, $\epsilon_n(\tau-1)$, $n = \{1, 2, 3, 4\}$, is a sufficient small step size at a certain iteration. The multipliers $\mu_{g,i}(\tau)$ and α_g are updated iteratively until the power allocated to weak user $i \in K_g$ is determined in compliance with the constraints (21b) and (21d), and the multipliers $\lambda_{\max,i}$ and $\nu_{\min,i}$ are updated to guarantee that the data rate of the weak user achieved by allocating P_w^* at $\mu_{g,i}^*$ and α_g^* is enough to satisfy its requirements. The overall algorithm iterates over power allocation until a closed-form solution is reached. It is worth pointing out that the same methodology can be easily followed to determine the power allocated to strong user $j \in K_g$ belonging to group g considering the constraint $P_s \leq P_s^T$ rather than the constraint $P_w > P_s^T$.

REFERENCES

- [1] H. Elgala, R. Mesleh, and H. Haas, "Indoor optical wireless communication: potential and state-of-the-art," *IEEE Communications Magazine*, vol. 49, no. 9, pp. 56–62, 2011.
- [2] M. Dehghani Soltani, E. Sarbazi, N. Bamiedakis, P. d. Souza, H. Kazemi, J. M. H. Elmirghani, I. H. White, R. V. Penty, H. Haas, and M. Safari, "Safety analysis for laser-based optical wireless communications: A tutorial," *Proceedings of the IEEE*, vol. 110, no. 8, pp. 1045–1072, 2022.
- [3] A. A. Qidan, M. Morales-Cespedes, T. El-Gorashi, and J. M. Elmirghani, "Resource allocation in laser-based optical wireless cellular networks," in *2021 IEEE Global Communications Conference (GLOBECOM)*, 2021, pp. 1–6.
- [4] A. A. Qidan, T. El-Gorashi, and J. M. H. Elmirghani, "Artificial neural network for resource allocation in laser-based optical wireless networks," in *ICC 2022 - IEEE International Conference on Communications*, 2022, pp. 3009–3015.
- [5] Y. Liu, Z. Qin, M. Elkashlan, Z. Ding, A. Nallanathan, and L. Hanzo, "Nonorthogonal multiple access for 5g and beyond," *Proceedings of the IEEE*, vol. 105, no. 12, pp. 2347–2381, 2017.
- [6] A. M. Abdelhady, O. Amin, A. Chaaban, B. Shihada, and M.-S. Alouini, "Downlink resource allocation for dynamic tdma-based vlc systems," *IEEE Transactions on Wireless Communications*, vol. 18, no. 1, pp. 108–120, 2019.
- [7] Y. Qiu, S. Chen, H.-H. Chen, and W. Meng, "Visible light communications based on cdma technology," *IEEE Wireless Communications*, vol. 25, no. 2, pp. 178–185, 2018.
- [8] S. S. Bawazir, P. C. Sofotasios, S. Muhandat, Y. Al-Hammadi, and G. K. Karagiannidis, "Multiple access for visible light communications: Research challenges and future trends," *IEEE Access*, vol. 6, pp. 26 167–26 174, 2018.
- [9] R. C. Kizilirmak, C. R. Rowell, and M. Uysal, "Non-orthogonal multiple access (noma) for indoor visible light communications," in *2015 4th International Workshop on Optical Wireless Communications (IWOW)*, 2015, pp. 98–101.
- [10] L. Yin, W. O. Popoola, X. Wu, and H. Haas, "Performance evaluation of non-orthogonal multiple access in visible light communication," *IEEE Transactions on Communications*, vol. 64, no. 12, pp. 5162–5175, 2016.
- [11] H. Marshoud, P. C. Sofotasios, S. Muhandat, G. K. Karagiannidis, and B. S. Sharif, "Error performance of noma vlc systems," in *2017 IEEE International Conference on Communications (ICC)*, 2017, pp. 1–6.
- [12] H. Kazemi, E. Sarbazi, M. Crisp, T. E. H. El-Gorashi, J. M. H. Elmirghani, R. V. Penty, I. H. White, M. Safari, and H. Haas, "A novel terabit grid-of-beam optical wireless multi-user access network with beam clustering," *IEEE Transactions on Communications*, pp. 1–1, 2025.
- [13] M. Zeng, A. Yadav, O. A. Dobre, G. I. Tsipopoulos, and H. V. Poor, "On the sum rate of mimo-noma and mimo-oma systems," *IEEE Wireless Communications Letters*, vol. 6, no. 4, pp. 534–537, 2017.
- [14] Q. Zhang, Q. Li, and J. Qin, "Robust beamforming for nonorthogonal multiple-access systems in miso channels," *IEEE Transactions on Vehicular Technology*, vol. 65, no. 12, pp. 10 231–10 236, 2016.
- [15] D. Chen, Z. Ren, Q. Wang, R. Hao, and J. Wang, "Resource allocation for slotted-enabled hybrid ofdma-noma vlc system," *IEEE Photonics Technology Letters*, vol. 37, no. 12, pp. 667–670, 2025.
- [16] X. Zhang, Q. Gao, C. Gong, and Z. Xu, "User grouping and power allocation for noma visible light communication multi-cell networks," *IEEE Communications Letters*, vol. 21, no. 4, pp. 777–780, 2017.
- [17] A. A. Qidan and et al., "Indoor laser-based wireless communications," in *Free Space Optics Technologies in B5G and 6G Era*. IntechOpen, 2024, ch. 2.
- [18] T. Gou, C. Wang, and S. A. Jafar, "Aiming perfectly in the dark-blind interference alignment through staggered antenna switching," *IEEE Transactions on Signal Processing*, vol. 59, no. 6, pp. 2734–2744, 2011.
- [19] M. Morales-Cespedes, O. A. Dobre, and A. Garcia-Armada, "Semi-blind interference aligned noma for downlink mu-miso systems," *IEEE Transactions on Communications*, vol. 68, no. 3, pp. 1852–1865, 2020.
- [20] M. Morales-Cespedes, M. C. Paredes-Paredes, A. Garcia Armada, and L. Vandendorpe, "Aligning the light without channel state information for visible light communications," *IEEE Journal on Selected Areas in Communications*, vol. 36, no. 1, pp. 91–105, 2018.
- [21] A. A. Qidan, M. Morales-Cespedes, A. G. Armada, and J. M. H. Elmirghani, "Resource allocation in user-centric optical wireless cellular networks based on blind interference alignment," *Journal of Lightwave Technology*, vol. 39, no. 21, pp. 6695–6711, 2021.
- [22] A. Adnan-Qidan, M. Morales Cespedes, and A. Garcia Armada, "User-centric blind interference alignment design for visible light communications," *IEEE Access*, vol. 7, pp. 21 220–21 234, 2019.
- [23] A. Adnan-Qidan, M. Morales-Cespedes, and A. G. Armada, "Load balancing in hybrid vlc and rf networks based on blind interference alignment," *IEEE Access*, vol. 8, pp. 72 512–72 527, 2020.
- [24] A. A. Qidan, T. El-Gorashi, and J. M. H. Elmirghani, "Cooperative artificial neural networks for rate-maximization in optical wireless networks," in *ICC 2023 - IEEE International Conference on Communications*, 2023, pp. 1143–1148.
- [25] H. Marshoud, V. M. Kapinas, G. K. Karagiannidis, and S. Muhandat, "Non-orthogonal multiple access for visible light communications," *IEEE Photonics Technology Letters*, vol. 28, no. 1, pp. 51–54, 2016.
- [26] Z. Yang, W. Xu, and Y. Li, "Fair non-orthogonal multiple access for visible light communication downlinks," *IEEE Wireless Communications Letters*, vol. 6, no. 1, pp. 66–69, 2017.
- [27] Q. Li, L. Shi, T. Tang, and Z. Xiong, "User cooperation and link selection in hybrid vlc/rf systems with noma," *IEEE Wireless Communications Letters*, vol. 13, no. 4, pp. 979–983, 2024.
- [28] S. Ma, Y. He, H. Li, S. Lu, F. Zhang, and S. Li, "Optimal power allocation for mobile users in non-orthogonal multiple access visible light communication networks," *IEEE Transactions on Communications*, vol. 67, no. 3, pp. 2233–2244, 2019.
- [29] M. Obeed, H. Dahrouj, A. M. Salhab, S. A. Zummo, and M.-S. Alouini, "User pairing, link selection, and power allocation for cooperative noma hybrid vlc/rf systems," *IEEE Transactions on Wireless Communications*, vol. 20, no. 3, pp. 1785–1800, 2021.
- [30] Z. Liu, F. Yang, J. Song, and Z. Han, "Multiple access for downlink multi-user vlc system: Noma or oma user pairing?" *IEEE Wireless Communications Letters*, vol. 12, no. 11, pp. 1916–1920, 2023.
- [31] Z. Wang, Q. Wang, S. Chen, and L. Hanzo, "An adaptive scaling and biasing scheme for ofdm-based visible light communication systems," *Opt. Express*, vol. 22, no. 10, pp. 12 707–12 715, May 2014.
- [32] R. Zhang, H. Claussen, H. Haas, and L. Hanzo, "Energy efficient visible light communications relying on amorphous cells," *IEEE Journal on Selected Areas in Communications*, vol. 34, no. 4, pp. 894–906, 2016.
- [33] J. P. G. Crouzeix and J. A. Ferland, "Algorithms for generalized fractional programming," *Math. Programm*, vol. 52, no. 3, pp. 191–207, 1991.
- [34] D. Bertsekas, *Convex Optimization Theory*, ser. Athena Scientific optimization and computation series. Athena Scientific, 2009.